A rising era of perovskite-based triple-junction photovoltaics

Hang Hu[1,2,*], Ting Pan[1,2], Ulrich W. Paetzold[1,2,*]

[1]Institute of Microstructure Technology (IMT), Karlsruhe Institute of Technology (KIT), Hermann-von-Helmholtz-Platz 1, 76344 Eggenstein-Leopoldshafen, Germany

[2]Light Technology Institute (LTI), Karlsruhe Institute of Technology (KIT), Engesserstrasse 13, 76131 Karlsruhe, Germany

*Correspondence: hang.hu@kit.edu (H.H.); ulrich.paetzold@kit.edu (U.W.P.)

Abstract

In a recent issue of *Nature*, Y. Hou and co-workers reported a certified record efficiency of 27.1% for triple-junction perovskite–perovskite–silicon photovoltaics. High open-circuit voltage is realized by the implementation of cyanate in the ultra-wide-bandgap perovskite (1.93 eV) top cell, achieving a uniform iodide–bromide distribution and minimized micro-strain inhomogeneity.

Multi-junction photovoltaics (PVs) efficiently optimize solar spectrum harvesting, *i.e.*, by mitigating inherent thermalization and transmission losses, to overcome the theoretical efficiency limit of single-junction solar cells (see Figure 1A). In the past decade, perovskite-based tandem solar cells demonstrated impressive progress, leading to record certified power conversion efficiencies (PCEs) > 29% for monolithic perovskite–silicon (Si) and perovskite–perovskite tandem solar cells, thereby exceeding by far the highest-ever reported efficiency for single-junction solar cells. Drawing inspiration from these advances, very recently, a handful of research groups demonstrated impressive advances in triple-junction all-perovskite and perovskite–perovskite–Si (3J PPS) solar cells[1–9] (see Figure 1B). These advances mark the beginning of a rising era of ultra-high-efficiency perovskite-based multi-junction PVs using three or even more junctions. The detailed balance limit in PCE of around ~45% for tandem solar cells increases up to ~51% for triple-junction solar cells.[2,5,8,9] Here, we focus on 3J PPS PVs. For this technology, which employ mature Si PV technology in the bottom cell, the detailed balance limit in PCE reaches 49.6% (Figure 1B),[5,7] bearing an enormous further potential to advance performance.

Advancing high-efficiency 3J PPS solar cells introduces additional complexity and several new challenges:[6,8] (1) the meticulous sequentially processing of high-quality multilayer stacks of perovskite and functional thin films on top of Si bottom solar cells (*e.g.*, the realization of low-loss interconnection junctions), (2) the processing of efficient and stable ultra-wide-bandgap (WBG) perovskite (E_g > 1.8 eV) top solar cells, (3) the improvement of stability, (4) the optimization of light management for maximizing current generation, and (5) the implementation of optimal bandgap combination (or the optimization of absorber thickness) of the three junctions for minimizing current mismatch. With regard to the latter, an early optical and electrical simulation was reported from H. J. Snaith and co-workers[10] in 2017, which revealed a practical potential in PCE (38.8%) with employing optimum bandgaps of 1.44 eV and 1.95 eV for the middle and top perovskites, respectively. However, high-quality middle-bandgap (MBG) perovskite with an optimum bandgap (1.4–1.5 eV) is based on an unstable Sn/Pb mixed composition. For this reason, all practical and experimental realization up to now compromised to a small extent to use slightly higher MBG (1.52–1.57 eV) perovskites.[1–9] In

2018, the first 3J PPS solar cells were demonstrated by J. Werner and co-workers[1] with addressing the processing challenge (1). Perovskite absorbers were fabricated on a textured surface of Si bottom cell using a sequential two-step method (*i.e.*, vapor deposition combined with spin coating), yielding an open-circuit voltage (V_{OC}) of 2.69 V and a PCE of 14.0%. However, imperfect interconnection junction (between the top and middle perovskite sub-cells, *i.e.*, challenge (1)) and the current mismatching (challenge (5)) led to a low fill factor (FF) < 0.7 and a short-circuit current density (J_{SC}) < 8 mA cm^{-2}. Until 2022, 3J PPS solar cells benefited from the utilization of self-assembled monolayers (SAM) as efficient hole-transport layers (especially at the interconnection junction between the top and middle perovskite cells, which is desired for (1)), pushing PCEs up to 20%–22.2% (Figure 1B).[2–4] Nevertheless, a large V_{OC} loss and phase instability in WBG (> 1.8 eV) perovskite top cell are critical factors (challenges (2) and (3)) hindering the improvement of 3J PPS solar cells, *i.e.*, > 40 mol% of bromide (Br^-) basically used in the mixed Br^-/iodide (I^-) halide composition results in severe photo-induced phase segregation and large non-radiative recombination losses. Meanwhile, in these 3J PPS solar cells, the MBG perovskite (~1.56 eV) middle cells were processed on top of the front-planar Si bottom cells, resulting in limited J_{SC} (< 10.5 mA cm^{-2}) and low total current generation (challenges (4) and (5)). Early in 2024, 3J PPS solar cells gained a significant momentum toward high PCEs > 24% (Figure 1B),[6–9] in which ultrahigh WBG (1.9–2.0 eV) perovskite top cells received a majority of research attention (desired for (2)).[6,7,9]

Recently, Y. Hou and colleagues[9] reported a landmark achievement in *Nature*, documenting a certified PCE of 27.1% for 3J PPS solar cells (Figure 1C). This PCE is the highest certified efficiency ever published for the technology, which is in par with Si solar cells, marking a significant breakthrough in the field. Their work demonstrates several breakthroughs that each addresses one of the major challenges ((2) to (5)) for advancing perovskite-based multi-junction PVs as described above:

Development of efficient and stable WBG perovskite top cell for maximizing V_{OC} (challenge (2)): The key innovation of Y. Hou and co-workers is the implementation of a previously unknown pseudohalide cyanate (OCN^-) in the WBG perovskite (1.93 eV)

top cell, which enables ultrahigh V_{OC} in WBG single-junction solar cells and, in turn, in 3J PPS solar cells. The integration of OCN^- into the WBG perovskite lattice resulted in improved thin-film uniformity and elevated defect formation energy. The OCN^- is shown to integrate perfectly into the lattice since its ionic radius and tolerance are well matched to those of Br^-, thereby providing a handle to regulate the crystallization process. Moreover, OCN^- ions integrated in the perovskite lattice effectively reduce the defects/mobile ion density and micro-strain inhomogeneity. This improvement facilitated to minimize the non-radiative recombination (reduced by ~71 mV for bulk non-radiative recombination loss). In consequent, a record V_{OC} of 1.422 V was demonstrated, enabling a high V_{OC} of 3.132 V in 3J PPS solar cells.

Improvement of stability (challenge (3)): It is highlighted that next to a very high PCE, these 3J PPS solar cells demonstrate an unprecedented long-term stability. After 700 h of testing under ISOS-D-3 conditions (a temperature of 65 °C and 85% relative humidity), the encapsulated 3J PPS solar cells maintained 96% of their initial PCE. Under the ISOS-L-3 test conditions, the encapsulated 3J PPS solar cells retained 80% of their initial PCE after 300 hours of exposure to AM 1.5G illumination. This improved stability in 3J is attributed to the suppressed phase segregation in WBG perovskite top cell.

Implementation of textured Si bottom cell for improving light management (challenge (4)): The perovskite middle and top cells were processed on top of the textured Si heterojunction bottom solar cell. With the benefit of this architecture, the light path enhancement given by the textured Si front surface results in an improved current generation (Figure 1C), *e.g.*, a high J_{SC} of 11.58 mA cm^{-2} in 3J PPS solar cells.

Utilization of thick MBG perovskite middle cell for minimizing current mismatch (challenge (5)): In previous literature, the current generation in the MBG perovskite solar cells limits the overall current of the 3J PPS solar cells. In response, the present article of Y. Hou and colleagues reported on an outstanding middle junction benefits

with reduced current mismatch in 3J architecture. A remarkable thick (~1.3 μm) MBG (1.55 eV) perovskite film contributed to the improvement of J_{SC} in middle junction (Figure 1C). Notably, despite the rather thick perovskite absorber layer, remarkably low V_{OC} losses were obtained in the MBG perovskite solar cells. We note that despite these innovations, a small current mismatch remains (*i.e.*, J_{SC} values of 12.22, 11.29, and 15.63 mA cm^{-2} for the top, middle, and bottom sub-cells, respectively), highlighting the further room for improvement.

In summary, we are at the start of a rising era of ultra-high-efficiency perovskite-based 3J PVs. The article by Y. Hou and co-workers demonstrates a millstone in this endeavor, with impressive innovations in (i) the performance of WBG perovskite top solar cells, (ii) remarkable long-term stability, (iii) the improved light management by implementing textured Si bottom solar cell, and (iv) the reduction of current mismatch losses by using very thick MBG perovskite solar cell. All these innovations will trigger new research in the field that benefits further from the ample learnings of the extensive research on perovskite-based tandem solar cells. To date, minimizing non-radiative recombination losses and improving phase stability for WBG perovskite solar cells remain the most critical challenges in further performance advances of perovskite-based 3J solar cells. Ultrahigh WBG (> 1.85 eV) perovskites need more exploration, such as processing control, compositional engineering, additive engineering, interfacial engineering, *etc.* In terms of MBG perovskite solar cells, up to now, non-optimum bandgaps (1.52–1.57 eV) limit the current generation in 3J PPS solar cells. By lowering the bandgap for MBG perovskite, *e.g.*, employing $FAPbI_3$ (~1.52 eV)[8] or Sn/Pb mixed perovskite (1.4–1.5 eV), the current matching can be improved. According to an idealized electrical and optical simulation reported recently from L. Restat *et al.*,[5] a practical efficiency potential of 44.3% is proposed with a perfect current matching (J_{SC} of ~14.1 mA cm^{-2} in the combination of 1.46 eV and 1.98 eV bandgaps for perovskites), which is over the practical potential of 39.3% for 2J PS solar cells. This delivers a promising roadmap for how 3J PPS solar cells outperform 2J PS solar cells.

ACKNOWLEDGMENTS

T.P. is grateful to thank financial support from the Chinese Scholarship Council (CSC). Financial support by Helmholtz Association (Project Zeitenwende, Solar Technology Acceleration Platform (Solar TAP), program oriented funding period IV of the Helmholtz Association (Materials and Technologies for the Energy Transition, Topic 1: Photovoltaics and Wind Energy, Code: 38.01.03)), and the Karlsruhe School of Optics and Photonics (KSOP) is gratefully acknowledged. The European Union co-funded the study (ERC, Lami-Pero, 101087673). Views and opinions expressed are, however, those of the author(s) only and do not necessarily reflect those of the European Union or the European Research Council. Neither the European Union nor the granting authority can be held responsible.

DECLARATION OF INTERESTS

The authors declare no competing interests.

REFERENCES

1. Werner, J., Sahli, F., Fu, F., Diaz Leon, J.J., Walter, A., Kamino, B.A., Niesen, B., Nicolay, S., Jeangros, Q., and Ballif, C. (2018). Perovskite/Perovskite/Silicon Monolithic Triple-Junction Solar Cells with a Fully Textured Design. ACS Energy Lett. *3*, 2052–2058.
2. Zheng, J., Wang, G., Duan, W., Mahmud, M.A., Yi, H., Xu, C., Lambertz, A., Bremner, S., Ding, K., Huang, S., et al. (2022). Monolithic Perovskite-Perovskite-Silicon Triple-Junction Tandem Solar Cell with an Efficiency of over 20%. ACS Energy Lett. *7*, 3003–3005.
3. Choi, Y.J., Lim, S.Y., Park, J.H., Ji, S.G., and Kim, J.Y. (2023). Atomic Layer Deposition-Free Monolithic Perovskite/Perovskite/Silicon Triple-Junction Solar Cells. ACS Energy Lett. *8*, 3141–3146.
4. Heydarian, M., Heydarian, M., Bett, A.J., Bivour, M., Schindler, F., Hermle, M., Schubert, M.C., Schulze, P.S.C., Borchert, J., and Glunz, S.W. (2023). Monolithic Two-Terminal Perovskite/Perovskite/Silicon Triple-Junction Solar Cells with Open Circuit Voltage >2.8 V. ACS Energy Lett. *8*, 4186–4192.
5. Restat, L., Messmer, C., Heydarian, M., Heydarian, M., Schoen, J., Schubert, M.C., and

Glunz, S.W. (2024). Optoelectrical Modeling of Perovskite/Perovskite/Silicon Triple-Junction Solar Cells: Toward the Practical Efficiency Potential. Sol. RRL *8*, 2300887.

6. Li, F., Wu, D., Shang, L., Xia, R., Zhang, H., Huang, Z., Gong, J., Mao, L., Zhang, H., Sun, Y., et al. (2024). Highly Efficient Monolithic Perovskite/Perovskite/Silicon Triple-Junction Solar Cells. Adv. Mater. *36*, 1–10.
7. Xu, F., Aydin, E., Liu, J., Ugur, E., Harrison, G.T., Xu, L., Vishal, B., Yildirim, B.K., Wang, M., Ali, R., et al. (2024). Monolithic perovskite/perovskite/silicon triple-junction solar cells with cation double displacement enabled 2.0 eV perovskites. Joule *8*, 224–240.
8. Hu, H., An, S.X., Li, Y., Orooji, S., Singh, R., Schackmar, F., Laufer, F., Jin, Q., Feeney, T., Diercks, A., et al. (2024). Triple-junction perovskite-perovskite-silicon solar cells with power conversion efficiency of 24.4%. Energy Environ. Sci. *17*, 2800–2814.
9. Liu, S., Lu, Y., Yu, C., Li, J., Luo, R., Guo, R., Liang, H., Jia, X., Guo, X., Wang, Y.D., et al. (2024). Triple-junction solar cells with cyanate in ultrawide-bandgap perovskites. Nature *628*, 306–312.
10. Hörantner, M.T., Leijtens, T., Ziffer, M.E., Eperon, G.E., Christoforo, M.G., McGehee, M.D., and Snaith, H.J. (2017). The Potential of Multijunction Perovskite Solar Cells. ACS Energy Lett. *2*, 2506–2513.

Figure 1. Triple-junction perovskite–perovskite–Si (3J PPS) solar cells

(A) Illustration of the use of the AM 1.5G spectrum by a 3J PPS solar cell. UV: ultraviolet; VIS: visible; IR: infrared; WBG: wide bandgap; BMG: middle bandgap; NBG: narrow bandgap.

(B) Historical evolution of the power conversion efficiencies (PCEs)[1–9] and the detailed balanced limit[5,7] of the 3J PPS solar cells.

(C) The schematic and cross-section scanning electron microscope images of the state-of-the-art 3J PPS solar cell based on the report of Y. Hou and co-workers.[9] The scale bar is 500 nm.

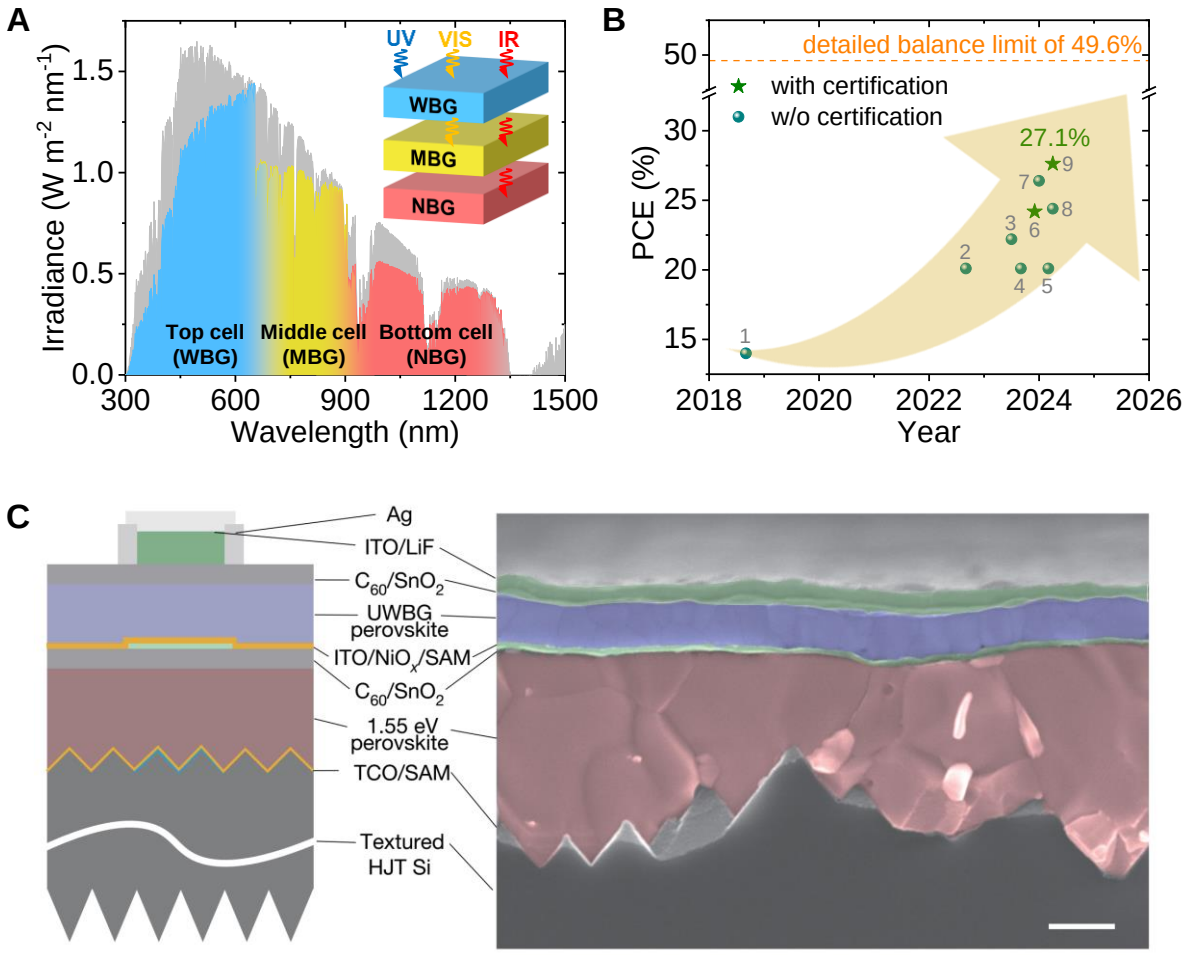
A
Irradiance (W m-2 nm-1)
Wavelength (nm)
UV
VIS
IR
WBG
MBG
NBG
Top cell (WBG)
Middle cell (MBG)
Bottom cell (NBG)
B
detailed balance limit of 49.6%
with certification
w/o certification
27.1%
PCE (%)
Year
C
Ag
ITO/LiF
C60/SnO2
UWBG perovskite
ITO/NiOx/SAM
C60/SnO2
1.55 eV perovskite
TCO/SAM
Textured HJT Si